

# INCREASING THE SPATIAL COVERAGE OF ATMOSPHERIC AEROSOL DEPTH MEASUREMENTS USING RANDOM FOREST AND MEAN FILTERS

Zhongying Wang<sup>1</sup>, Rafael Pires de Lima<sup>1</sup>, James L. Crooks<sup>2</sup>, Elizabeth Anne Regan<sup>2</sup>, Morteza Karimzadeh<sup>1</sup>

<sup>1</sup> Department of Geography, University of Colorado Boulder

<sup>2</sup> National Jewish Health

## ABSTRACT

Aerosols play a critical role in atmospheric chemistry, and affect clouds, climate, and human health. However, the spatial coverage of satellite-derived aerosol optical depth (AOD) products is limited by cloud cover, orbit patterns, polar night, snow, and bright surfaces, which negatively impacts the coverage and accuracy of particulate matter modeling and health studies relying on air pollution characterization. We present a random forest model trained to capture spatial dependence of AOD and produce higher coverage through imputation. By combining the models with and without the mean filters, we are able to create full-coverage high-resolution daily AOD in the conterminous U.S., which can be used for aerosol estimation and other studies leveraging air pollutant concentration levels.

**Index Terms**— Aerosol Optical Depth, Random Forest, Imputation

## 1. INTRODUCTION

Aerosols are suspensions of particles in gas, with sizes ranging from  $10^{-9}$  to  $10^{-4}$ m. They originate from various sources such as urban/industrial emissions, biomass burning, gaseous precursors, sea salt, and dust [1]. Aerosols have a crucial role in regional and global climate systems, affecting radiation budget, cloud formation, atmospheric circulation, and surface temperature [2]. Ground-level aerosols, particularly PM<sub>10</sub> (Particulate Matter with diameter  $\leq 10\mu m$ ) and PM<sub>2.5</sub> (diameter  $\leq 2.5\mu m$ ), are linked to adverse health effects like asthma, stroke, heart disease, and pregnancy complications [3][4]. Hence, understanding aerosol variations is vital for climate change and public health research. Aerosol Optical Depth (AOD) measures aerosols in a column of air

and is commonly used to estimate PM levels [5][6]. While the Aerosol RObotic NETwork (AERONET) provides distributed observations of spectral AOD [7], the point-based observations lack the high-resolution spatial coverage of remote sensing. Satellite-derived AOD products provide a solution for high-resolution AOD retrieval, and the multiangle implementation of atmospheric correction (MAIAC) AOD are commonly used in characterizing spatiotemporal variations of aerosols [8] and estimating surface PM levels [9]. However, the coverage of satellite-derived AOD is limited by cloud cover, snow cover, and surface brightness [10].

A variety of methods have been developed to gap-fill AOD by incorporating external information, including geostatistical methods and machine learning (ML). ML methods show high performance and computing efficiency, but mainly rely on the relationships in the feature space and ignore the spatial dependence. In this study, we incorporate spatial information into a random forest model to impute the missing AOD values and provide a high-resolution full-coverage AOD. To increase the spatial coverage of AOD and utilize spatial dependency, we apply mean filters to the AOD data. The available MAIAC AOD was used as the target variable, and external information (including meteorological variables, elevation, wildfire smoke, and NDVI) was used as predictors. We assessed the AOD imputation performance between the random forest model with and without mean filters.

## 2. MATERIALS AND METHODS

### 2.1. Materials

#### 2.1.1. Satellite-Retrieved Product

The MODIS MAIAC algorithm retrieves daily AOD at 1 km spatial resolution from the MODIS Aqua and Terra sensor. Compared with old DT and DB algorithms, MAIAC improves the coverage on both dark vegetation and bright deserts and increase the spatial resolution. We obtained 16 MODIS Sinusoidal tiles of MAIAC AOD covering the conterminous U.S. from 2005 to 2021 from the NASA website<sup>1</sup>. The MCD19A2 AOD data product contains two bands of AOD measurements:

<sup>1</sup><https://lpdaac.usgs.gov/products/mcd19a2v006/>

blue band AOD at  $0.47\mu m$  and green band AOD at  $0.55\mu m$ . We used both as target variables in the evaluation.

In addition, a MODIS Combined 16-Day Normalized Difference Vegetation Index (NDVI) at 1 km resolution, which is generated from the MODIS/006/MCD43A4 surface reflectance composites, was retrieved via Google Earth Engine. To align with the daily AOD image, the closest date's NDVI image is associated with the AOD.

### 2.1.2. Meteorological Data and Elevation Data

We obtained meteorological data from Daymet [11] and gridMET [12]. The Daymet dataset includes minimum and maximum temperature, precipitation, shortwave radiation, vapor pressure, day length. The dataset covers our study period from 2005 to 2021, and is at a  $1km \times 1km$  spatial resolution and a daily temporal resolution. To account for the wind impact on aerosol dispersion, we also obtained wind direction and wind velocity variables from gridMET, a dataset of daily high-spatial resolution (4 km, 1/24th degree) surface meteorological data. The two gridMET variables are resampled and aligned with other 1 km resolution variables.

A 1km resolution elevation dataset is obtained from Earth-Env<sup>2</sup>, which is derived from the digital elevation model product of global 250m GMTED2010 and near-global 90 m SRTM4.1dev [13].

### 2.1.3. Wildfire Smoke Data

NOAA Satellite Analysis Branch's Hazard Mapping System (HMS) combines near real-time polar and geostationary satellite observations into a common framework in which expert image analysts perform quality control of automated fire products and digitization of smoke plumes. HMS's smoke analysis is based on visual classification of plumes using GOES-16 and GOES-17 ABI true-color imagery, and the smoke attributes are used to outline the smoke polygon and plume density. The density information is qualitatively described using light, medium, and heavy labels that are assigned based on the apparent thickness (opacity) of the smoke in the satellite imagery.

The daily wildfire smoke polygon dataset is retrieved from NOAA website<sup>3</sup>, and the data available date is from August 5th, 2005, until now.

### 2.1.4. Spatial and Temporal Encoding

The spatial and temporal encoding variables included the coordinate (latitude and longitude), year, and temporal cyclical features encoding (Cosine and Sine of month and day of the year). The spatial and temporal encodings are designed to capture the spatial and temporal variability of AOD.

<sup>2</sup><http://www.earthenv.org/topography>

<sup>3</sup><https://www.ospo.noaa.gov/Products/land/hms.html#data>

## 2.2. Methods

### 2.2.1. Mean Filters

A mean filter is commonly used in image processing, and is designed to reduce the amount of intensity variations between neighboring pixel values and reduce noise in images. We use mean filters to increase the spatial coverage of AOD data with high rates of missingness, and capture spatial information of neighboring pixels based on the first law of geography [14].

Mean filtering can be considered a convolution filter, and the average of the values in the local neighborhood replaces the value of each pixel. This is presented as the following equation:

$$g(x, y) = \frac{1}{n} \sum_{(i, j) \in S} f(i, j)$$

where  $g(x, y)$  is the smoothed image derived from the original image  $f(i, j)$ .  $S$  is the neighborhood set of  $(x, y)$  and  $n$  is the number of non-null values in  $S$ . Fig.1 shows an example of a mean-filtered AOD image.

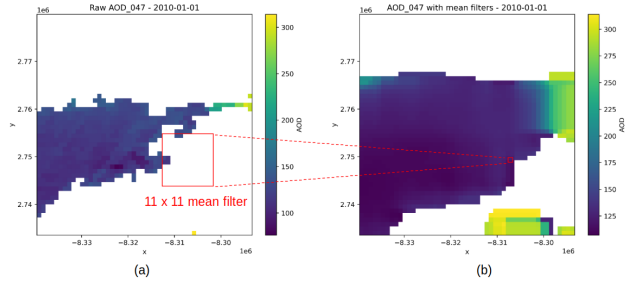


**Fig. 1.** Example of Mean Filters. (a) Raw green band AOD. (b) Mean-filtered green band AOD

We applied  $11 \times 11$  mean filters to the MAIAC AOD data for both green and blue bands, and gained about 15% increase in the spatial coverage.

### 2.2.2. Random Forest

Random Forest (RF) is an ensemble learning algorithm that combines multiple base learners to make collective predictions [15]. By aggregating the outputs of several individual models, RF can capture non-linear relationships and enhance the algorithm's accuracy and generalization capabilities. Recently, it has been commonly used in AOD imputation and PM2.5 concentration estimations [16]. In this study, we employed the RF with mean filters to impute daily AOD values for the conterminous U.S., showing the improvement of the mean filters.

The construction of RF regression model involves two primary steps: (1) random subspace selection and (2) ensemble

aggregation. For (1), a subset of features is randomly selected for each decision tree and such randomness promotes diversity among the trees, enabling the model to capture different aspects of the data. In (2), the predictions from individual decision trees are combined using averaging to produce the final prediction. The ensemble strategy enhances the model's stability, accuracy, and ability to handle high-dimensional data.

### 2.2.3. Training and Evaluation

For each day from August 5th, 2005, to December 31st, 2021, data points located at EPA's monitoring stations are used to train the RF models. The MAIAC AOD at blue and green bands are set as target variables and multiplied by a scale factor of 1000. We used random search cross-validation (CV) to fine-tune the hyperparameters of RF, including the number of trees, the maximum depth of the tree, the minimum number of samples required to split an internal node, the minimum number of samples required to be at a leaf node, and the number of features to consider when looking for the best split.

To better validate the performance of the model, three kinds of 5-fold CV were deployed, including random CV, spatial CV, and temporal CV. In random CV, samples are randomly divided into training and testing. 80% of samples were used for model training and hyperparameters tuning, and the remaining samples were held out for independent validation. Spatial CV separates the dataset based on the location of the sites to account for spatial autocorrelation and help prevent overfitting. Similarly, temporal CV divides the dataset into training and testing according to the date, and accounts for temporal autocorrelation.

In the evaluation, the coefficient of determination ( $R^2$ ), Root Mean Square Error (RMSE), and Mean Bias Error (MBE) were used as the performance metrics.

## 3. RESULTS AND DISCUSSIONS

During the study period, the daily coverage of MAIAC AOD in the conterminous U.S. remained at an average of approximately 40%. The highest coverage month was September, reaching 59%, and the lowest was February, with a coverage rate of 29%. After applying the  $11 \times 11$  mean filters, the coverage increased to 76% in September and 41% in February. The coverage of AOD has a high spatial heterogeneity, with higher rates in states having fewer cloudy days (e.g., California, Arizona, and New Mexico) and lower rates in northern states (e.g., Maine, Michigan, and Minnesota).

Imputed AOD values of two bands from models with and without mean filters were separately compared with MAIAC AOD retrievals to quantify the model performance. Table 1 summarizes the statistics of held-out validation results. Overall, the results of both blue and green bands demonstrate that the models with mean filters are much better than models without mean filters in all the evaluation metrics, including

in spatial and temporal validation, with a much higher  $R^2$ , lower RMSE, and MBE closer to MBE. These results indicate that the models with mean filters are more robust with spatial and temporal autocorrelation and are less biased than those without mean filters. The average AOD of neighboring pixels has been proven to be a critical feature in the imputation. The neighboring average AOD of two bands ranks the top two in the feature importance (about 0.41), followed by the wildfire smoke density (about 0.06).

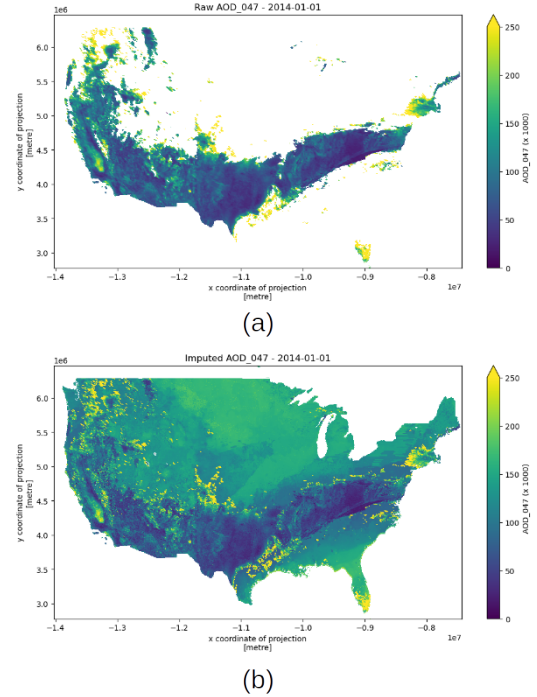


**Fig. 2.** Example of results in the conterminous U.S. on Jan 1st, 2014. (a) Raw green band AOD. (b) Imputed green band AOD.

By overlapping the two model outputs, with and without the mean filters (for places where mean-filtering does is unavailable due to lack of data in the  $11 \times 11$  window), we can obtain the full coverage of AOD in the conterminous U.S. (Fig.2)

## 4. CONCLUSIONS

We proposed a random forest method with mean filters to capture the spatial dependence of AOD to impute the missing data of AOD. According to the random, spatial and temporal validation, the models with mean filters are confirmed to have higher performance and less bias than the models without mean filters. By combining the models with and without mean filters, we can obtain full spatial coverage AOD in the conterminous U.S. The study has important implications for

**Table 1.** Comparison of Model Performance for MAIAC AOD Imputation.

|                           | Random Validation |        |       | Spatial Validation |        |       | Temporal Validation |        |        |
|---------------------------|-------------------|--------|-------|--------------------|--------|-------|---------------------|--------|--------|
|                           | R2                | RMSE   | MBE   | R2                 | RMSE   | MBE   | R2                  | RMSE   | MBE    |
| AOD 047 with mean filters | 0.97              | 36.23  | 0.10  | 0.96               | 40.91  | -0.40 | 0.94                | 36.44  | -0.31  |
| AOD 047 w/o mean filters  | 0.61              | 132.08 | -0.09 | 0.48               | 138.21 | 1.78  | 0.29                | 151.54 | -17.53 |
| AOD 055 with mean filters | 0.97              | 25.97  | 0.07  | 0.95               | 28.20  | 1.08  | 0.95                | 33.33  | -0.82  |
| AOD 055 w/o mean filters  | 0.63              | 94.81  | 0.08  | 0.42               | 124.45 | -2.02 | 0.30                | 111.53 | -7.85  |

the imputation of AOD and extensive applications of high-resolution MAIAC AOD data.

## 5. ACKNOWLEDGMENTS

This work was supported through NIH grant R21ES032973, and supported through the University of Colorado Population Center (CUPC) funded by Eunice Kennedy Shriver National Institute of Child Health & Human Development of the National Institutes of Health (P2CHD066613).

## 6. REFERENCES

- [1] G. Myhre, C. Myhre, B. Samset, and T. Storelvmo, "Aerosols and their relation to global climate and climate sensitivity," *Nature Education Knowledge*, vol. 4, no. 5, p. 7, 2013.
- [2] Z. Li, X. Xia, M. Cribb, W. Mi, B. Holben, P. Wang, H. Chen, S.-C. Tsay, T. Eck, F. Zhao *et al.*, "Aerosol optical properties and their radiative effects in northern china," *Journal of Geophysical Research: Atmospheres*, vol. 112, no. D22, 2007.
- [3] P. M. Mannucci and M. Franchini, "Health effects of ambient air pollution in developing countries," *International journal of environmental research and public health*, vol. 14, no. 9, p. 1048, 2017.
- [4] X. Yu, M. M. Rahman, Z. Wang, S. A. Carter, J. Schwartz, Z. Chen, S. P. Eckel, D. Hackman, J.-C. Chen, A. H. Xiang *et al.*, "Evidence of susceptibility to autism risks associated with early life ambient air pollution: a systematic review," *Environmental Research*, vol. 208, p. 112590, 2022.
- [5] J. Li, X. Ge, Q. He, and A. Abbas, "Aerosol optical depth (aod): spatial and temporal variations and association with meteorological covariates in taklimakan desert, china," *PeerJ*, vol. 9, p. e10542, 2021.
- [6] M. Ghahremanloo, Y. Choi, A. Sayeed, A. K. Salman, S. Pan, and M. Amani, "Estimating daily high-resolution pm2. 5 concentrations over texas: Machine learning approach," *Atmospheric Environment*, vol. 247, p. 118209, 2021.
- [7] B. N. Holben, T. F. Eck, I. a. Slutsker, D. Tanré, J. Buis, A. Setzer, E. Vermote, J. A. Reagan, Y. Kaufman, T. Nakajima *et al.*, "Aeronet—a federated instrument network and data archive for aerosol characterization," *Remote sensing of environment*, vol. 66, no. 1, pp. 1–16, 1998.
- [8] G. de Leeuw, C. Fan, Z. Li, J. Dong, Y. Li, Y. Ou, and S. Zhu, "Spatiotemporal variation and provincial scale differences of the aod across china during 2000–2021," *Atmospheric Pollution Research*, vol. 13, no. 4, p. 101359, 2022.
- [9] Q. Di, I. Kloog, P. Koutrakis, A. Lyapustin, Y. Wang, and J. Schwartz, "Assessing pm2. 5 exposures with high spatiotemporal resolution across the continental united states," *Environmental science & technology*, vol. 50, no. 9, pp. 4712–4721, 2016.
- [10] A. Lyapustin and Y. Wang, "Modis multi-angle implementation of atmospheric correction (maiac) data user's guide," *NASA: Greenbelt, MD, USA*, vol. 6, no. June, pp. 1–19, 2018.
- [11] M. Thornton, R. Shrestha, Y. Wei, P. Thornton, S. Kao, and B. Wilson, "Daymet: daily surface weather data on a 1-km grid for north america, version 4 r1," *ORNL DAAC, Oak Ridge, Tennessee, USA. Single Pixel Extraction Tool—Daymet (ornl.gov)*, 2022.
- [12] J. T. Abatzoglou, "Development of gridded surface meteorological data for ecological applications and modelling," *International Journal of Climatology*, vol. 33, no. 1, pp. 121–131, 2013.
- [13] G. Amatulli, S. Domisch, M.-N. Tuanmu, B. Parmentier, A. Ranipeta, J. Malczyk, and W. Jetz, "A suite of global, cross-scale topographic variables for environmental and biodiversity modeling," *Scientific data*, vol. 5, no. 1, pp. 1–15, 2018.
- [14] W. R. Tobler, "A computer movie simulating urban growth in the detroit region," *Economic geography*, vol. 46, no. sup1, pp. 234–240, 1970.
- [15] L. Breiman, "Random forests," *Machine learning*, vol. 45, pp. 5–32, 2001.

- [16] Z.-Y. Chen, J.-Q. Jin, R. Zhang, T.-H. Zhang, J.-J. Chen, J. Yang, C.-Q. Ou, and Y. Guo, "Comparison of different missing-imputation methods for maiac (multiangle implementation of atmospheric correction) aod in estimating daily pm<sub>2.5</sub> levels," *Remote Sensing*, vol. 12, no. 18, p. 3008, 2020.